

# The role of thermal conduction in magnetized viscous-resistive ADAFs

J. Ghanbari<sup>1\*</sup>, S. Abbassi<sup>2,3†</sup> and M. Ghasemnezhad<sup>1</sup>

<sup>1</sup>*Department of Physics, School of Sciences, Ferdowsi University of Mashhad, Mashhad, 91775-1436, Iran*

<sup>2</sup>*School of Physics, Damghan University of Basic Sciences, P.O.Box 36715-364, Damghan, Iran*

<sup>3</sup>*School of Astronomy, Institute for Research in Fundamental Sciences (IPM), P.O.Box 19395-5531, Tehran, Iran*

## ABSTRACT

Observations of the hot gas, which is surrounding Sgr A\* and a few other nearby galactic nuclei, imply that mean free paths of electron and proton are comparable to gas capture radius. So, hot accretion flows likely proceed under weak collision conditions. As a result thermal conduction by ions has a considerable contribution in transfer of the realized heat in accretion mechanisms. We study a 2D advective accretion disk bathed in a poloidal magnetic field of a central accretor in the presence of thermal conduction. We find self-similar solutions for an axisymmetric, rotating, steady, viscose-resistive, magnetized accretion flow. The dominant mechanism of energy dissipation is assumed to be turbulence viscosity and magnetic diffusivity due to magnetic field of the central accretor. We show that the global structure of ADAFs are sensitive to viscosity, advection and thermal conduction parameters. We discuss how radial flow, angular velocity and density of accretion flows may vary with the advection, thermal conduction and viscous parameters.

**Key words:** accretion, accretion flow, magnetic field, magnetohydrodynamics: MHD

## 1 INTRODUCTION

The foundations of our present understanding about advection dominated accretion flows were laid out in a series of papers by Narayan & Yi (1994,1995 a,b), although some ideas were anticipated much earlier by Ichimaru (1977). The specific abbreviation ADAF, which stands for advection dominated accretion flow, was introduced by Lasota et al. (1996). An ADAF is defined as one in which a large fraction of the viscously generated heat is advected with the accreting gas, and only a small fraction of the energy is radiated. ADAFs have an opposite regime in comparison with the standard model. In the standard model, flow is described in away that the heat generated by the viscosity radiates out of the system immediately after its generation (Shakura & Sunyaev 1973).

These advection-dominated accretion flows occur in two regimes depending on their mass accretion and optical depth. Actually the optical depth of accretion flows is highly dependent on accretion rates. In a high mass accretion rate, the optical depth becomes very high and the radiation generated by the accretion flow can be trapped within the disk. This type of accretion disks is known as optically thick or Slim Disks which has been introduced by Abramowicz et al.

(1998). In the limit of low mass accretion rate, the disk becomes optically thin. In this case, the cooling time of accretion flows is longer than accreting time scale. So the energy generated by accretion flows mostly remains in the disks and the disks can not radiate their energies efficiently. This kind of accretion flows are named radiation inefficient accretion flows (RIAFs). This type of accretion flows is investigated by many authors (Narayan & Yi 1994, Abramowicz et al. 1995, Chen 1995).

These types of solutions have been used to interpret the spectra of X-ray binary black holes in their quiescent or low/hard state as an alternative to the Shapiro, Lightman and Eardly (1976, SLE) solutions. Since ADAFs have large radial velocities and also the infalling matter carries the thermal energy to the black hole, the energy transported by advection can stabilize the thermal instability by removing their steep temperature gradient; thus the ADAF models have been widely used to explain the observations of low luminous observed in Sgr A\* (Narayan et al. 1996, Hameuray et al. 1997). However, numerical simulations of radiation inefficient accretion flows revealed that the low viscous flows are convectively unstable and therefore convection strongly influences the global structure of accretion flows (Igumenshchev, Abramowicz & Narayan 2000). Thus, another type of accretion flows was proposed, in which the convection plays a dominant mechanism in transporting the energy, an-

\* E-mail: ghanbari@ferdowsi.um.ac.ir

† E-mail: sabbassi@dubs.ac.ir

gular momentum and local released viscose energy within the disk.

A remarkable problem arises when the accretion disks threaded by a magnetic field. In the ADAF models, the temperature of accreting disks is so high that the accreting materials are ionized. So, the magnetic field plays an important role in the dynamics of the accretion flows. Some authors tried to solve the MHD equations of magnetized ADAFs analytically. For example, Kaburaki (2000) has presented a set of analytical solutions for a fully advective accretion flow in a global magnetic field. Shadmehri (2004) has extended this analysis for a non-constant resistivity. Ghanbari et al. (2007) have presented a set of self-similar solutions for 2D viscous-resistive advection dominated accretion flows (ADAFs) in the presence of dipolar magnetic field of the central accretor. They have shown that the presence of magnetic field and its associated resistivity can considerably change the picture of the accretion flows.

Recent observations of hot accretion flows around active galactic nuclei indicate that they should be based on the collisionless regimes.

Chandra observations provide tight constraints on both density and temperature of gas at or near the Bondi capture radius in Sgr A\* and several other nearby galactic nuclei. Tanaka & Menou (2006) with some calculations have shown that the accretion disks in such systems will proceed under weakly-collisional conditions. So, the thermal conduction has an important role in the energy transport along the disks. The aim of this work is to consider the effect of thermal conduction which has been largely neglected before, as an energy transport mechanism, on the 2D structure of ADAFs. It could affect the global properties of hot accretion flows substantially. A few authors considered the role of turbulent heat transport in ADAF disks (Honma 1996 , Manmoto et al.2000). Since thermal conduction acts to oppose the formation of temperature gradient that causes it, one might expect that the temperature and density profiles for accretion flows are modified in which thermal conduction plays a significant role to appear different, compared to those flows which thermal conduction is less effective (Shadmehri 2008).

The weakly-collisions nature of hot accretion flows has been addressed previously (Mahadevan & Quataret 1997). Johanson & Quataret (2007) studied the effect of electron thermal conduction on the properties of hot accretion flows under the assumption of spherical symmetry. In another interesting analysis, Tanaka & Menou (2006), studied the effect of saturated thermal conduction on optically thin ADAFs using an extension of self-similar solution of Narayan & Yi (1994). In their solutions, the thermal conduction is provided an extra degree of freedom which affects the global dynamical behaviors of the accretion flow. Abbassi et al. (2008) have presented a set of self-similar solutions for ADAFs with a toroidal magnetic field in which the saturated thermal conduction has a great role in the energy transport in the radial direction. The tangled magnetic field in accretion flows would likely reduce the effective mean free paths of particles. The magnitude of this reduction which depends on the magnetic field geometry, is still unknown. We have accounted this possibility by allowing the value of saturated constant,  $\phi_s$ , to vary in our solutions. Magnetic field also has an important role for transferring angular mo-

mentum along the disks. So the dynamical structure of the disk will be affected by magnetic field strength and configuration. So investigating the magnetized accretion flow with thermal conduction is an important issue.

## 2 THE BASIC EQUATIONS

We describe the 2-D hot accretion flow with similar maner of Narayan & Yi (1995). We adopt spherical polar coordinates  $(r, \theta, \phi)$  for axi-symmetric and steady state flows ( $\frac{\partial}{\partial \phi} = \frac{\partial}{\partial t} = 0$ ).The fundamental MHD governing equations can be written as:

The equation of continuity gives

$$\frac{D\rho}{Dt} + \rho \nabla \cdot \mathbf{u} = 0 \quad (1)$$

The equation of motion

$$\rho \frac{D\mathbf{u}}{Dt} = -\nabla P - \rho \nabla \phi - \mu \nabla^2 \mathbf{u} + (\mu_b + \frac{1}{3}\mu) \nabla(\nabla \cdot \mathbf{u}) + \frac{1}{4\pi} \mathbf{J} \times \mathbf{B} \quad (2)$$

The equation of energy

$$\rho [\frac{D\epsilon}{Dt} + P \frac{D}{Dt} (\frac{1}{\rho})] = Q_{vis} + Q_B - Q_{rad} + Q_{cond} \quad (3)$$

Gauss's law

$$\nabla \cdot \mathbf{B} = 0 \quad (4)$$

and the induction equation

$$\frac{D\mathbf{B}}{Dt} = \nabla \times (\mathbf{u} \times \mathbf{B}) + \eta \nabla^2 \mathbf{B} \quad (5)$$

where  $\rho$  is the density of the gas,  $p$  the pressure,  $\epsilon$  the internal energy,  $\mathbf{u}$  is the flow velocity,  $\mathbf{B}$  is the the magnetic field,  $\mathbf{J} = \nabla \times \mathbf{B}$  the current density,  $\eta$  the magnetic diffusivity in which for simplicity it is assumed to be a constant parameter (see, e.g., Kaburaki 2000),  $\mu$  and  $\mu_b$  are the shear and bulk viscosities .

The viscous heating rate is defined as the expression:

$$Q_{vis} = 2\mu E_{ij} E^{ij} + (\mu_b - \frac{2}{3}\mu) (\nabla \cdot \mathbf{v})^2 \quad (6)$$

where  $E_{ij} = \frac{1}{2}(v_{i,j} + v_{j,i})$  is a symmetric tensor and is known as the rate of the strain tensor.

We have adopted saturated conduction (Cowie & Mckee 1977) as:

$$Q_{cond} = -\nabla \cdot F_s \quad (7)$$

where as we have already mentioned  $F_s = 5\phi_s \rho c_s^3$  is the saturated conduction flux on the direction of the temperature gradient. Tanka & Menou (2006) have shown that for very small  $\phi_s$  their solutions coincide the standard ADAF solutions. **They have shown that** by adding the saturated conduction parameter,  $\phi_s$ , the effect of thermal conduction can be better seen when we will approach to  $\sim 0.001 - 0.01$ . So, we have investigated the effect of thermal conduction in this range.

So, magnetic reconnection may lead to energy release. Also, we can consider the viscous and resistive dissipations due to a turbulence cascade. In this study, the resistive dissipation is defined:

$$Q_B = \frac{\eta}{4\pi} J^2 \quad (8)$$

In the right hand side of the energy equation we have:

$$Q_+ - Q_- + Q_{cond} = Q_{adv} = fQ_+ + Q_{cond}$$

where  $Q_+ = Q_{vis} + Q_B$ ,  $Q_- = Q_{rad}$  and  $Q_{adv}$  represents the advective transport of energy and is defined as the difference between the magneto-viscous heating rate,  $Q_+$ , and radiative cooling rate,  $Q_{rad}$  plus the energy transport by conduction,  $Q_{cond}$ . We employ the parameter  $f = 1 - \frac{Q_-}{Q_+}$  to measure the high degree to which accretion flow is advection-dominated. When  $f \sim 1$  the radiation can be neglected and the accretion flow is advection dominated while in the case of small  $f$  the disk is in the radiation dominated case. So we can rearrange the right hand side of the energy equation to  $fQ_+ + Q_{cond}$ , where  $f \leq 1$ . In general, it varies with  $r$  and depends on the details of heating and cooling processes. For simplicity, it is assumed to be a constant.

For simplicity, the self-gravity of the disc and the effect of general relativity have been neglected. Also, we neglect radiation pressure in the equations because in optically thin ADAFs,  $P^{gas} \gg P^{rad}$ . We adopt the dipolar configuration for the magnetic field. Also we have neglected the  $\theta$ -component of the flow velocity  $u_\theta = 0$ , and the bulk viscosity of the flow,  $\mu_b = 0$ . Now, we formulate the basic equations (1)-(5) in spherical polar coordinates as follows:

$$\frac{\partial \rho}{\partial t} + \frac{1}{r^2} \frac{\partial}{\partial r}(r^2 \rho u_r) + \frac{1}{r} \frac{\partial}{\partial \theta}(\rho u_\theta) = 0, \quad (9)$$

The three components of the momentum equations give (e.g., Mihalas & Mihalas 1984): r component

$$\begin{aligned} \rho[u_r \frac{\partial u_r}{\partial r} - \frac{u_\varphi^2}{r}] &= -\frac{GM\rho}{r^2} - \frac{\partial p}{\partial r} + \mu[\frac{4}{3} \frac{\partial^2 u_r}{\partial r^2} + \frac{8}{3} \frac{1}{r} \frac{\partial u_r}{\partial r} \\ &- \frac{8}{3} \frac{u_r}{r^2} + \frac{1}{r^2} \cot \theta \frac{\partial u_r}{\partial \theta} + \frac{1}{r^2} \frac{\partial}{\partial \theta}(\frac{\partial u_r}{\partial \theta})] \\ &+ \frac{1}{4\pi}[-\frac{B_\theta}{r}(\frac{\partial}{\partial r}(rB_\theta) - \frac{\partial B_r}{\partial \theta}) - \frac{B_\varphi}{r} \frac{\partial}{\partial r}(rB_\varphi)] \end{aligned} \quad (10)$$

$\theta$  component

$$\begin{aligned} \rho[-\frac{\cot \theta}{r} u_\varphi^2] &= -\frac{1}{r} \frac{\partial P}{\partial \theta} + \mu[\frac{8}{3} \frac{1}{r^2} \frac{\partial u_r}{\partial \theta} + \frac{1}{3} \frac{1}{r} \frac{\partial^2 u_r}{\partial r \partial \theta}] \\ &+ \frac{1}{4\pi}[\frac{B_r}{r}(\frac{\partial}{\partial r}(rB_\theta) - \frac{\partial B_r}{\partial \theta}) - \frac{B_\varphi}{r \sin \theta} \frac{\partial}{\partial \varphi}(B_\varphi \sin \theta)] \end{aligned} \quad (11)$$

$\varphi$  component

$$\begin{aligned} \rho[u_r \frac{\partial u_\varphi}{\partial r} + \frac{u_r u_\varphi}{r}] &= \mu[\frac{\partial^2 u_\varphi}{\partial r^2} + \frac{2}{r} \frac{\partial u_\varphi}{\partial r} + \frac{1}{r^2} \cot \theta \frac{\partial u_\varphi}{\partial \theta} \\ &+ \frac{1}{r^2} \frac{\partial^2 u_\varphi}{\partial \theta^2} - \frac{u_\varphi}{r^2 \sin^2 \theta}] + \frac{1}{4\pi}[B_\theta(\frac{1}{r \sin \theta} \frac{\partial}{\partial \theta}(\sin \theta B_\varphi) \\ &+ \frac{B_r}{r} \frac{\partial}{\partial r}(rB_\varphi)] \end{aligned} \quad (12)$$

the equation of energy

$$\begin{aligned} \rho[u_r \frac{\partial \varepsilon}{\partial r} - \frac{P u_r}{\rho^2} \frac{\partial \rho}{\partial r}] &= -\frac{2}{3} \mu f [\frac{1}{r^2} \frac{\partial}{\partial r}(r^2 u_r)]^2 + 2\mu f [(\frac{\partial u_r}{\partial r})^2 \\ &+ 2(\frac{u_r}{r})^2 + \frac{1}{2}(\frac{1}{r} \frac{\partial u_r}{\partial \theta})^2 + \frac{1}{2}[r \frac{\partial}{\partial r}(\frac{u_r}{r})]^2 + \frac{1}{2}[\frac{\sin \theta}{r} \frac{\partial}{\partial \theta}(\frac{u_\varphi}{\sin \theta})]^2 \\ &] + \frac{\eta}{4\pi r^2} [\frac{\partial}{\partial r}(rB_\theta) - \frac{\partial B_r}{\partial \theta}]^2 - \frac{1}{r^2} \frac{\partial}{\partial r}(5\Phi_s r^2 P^{3/2} \rho^{-1/2}) \\ &- \frac{1}{r \sin \theta} \frac{\partial}{\partial \theta}(5\Phi_s \sin \theta P^{3/2} \rho^{-1/2}) \end{aligned} \quad (13)$$

The three components of the induction equation

$$u_r \frac{\partial B_r}{\partial r} = \frac{\partial}{\partial \theta} [r \sin \theta (u_r B_\theta - \frac{\eta}{r} [\frac{\partial}{\partial r}(rB_\theta) - \frac{\partial B_r}{\partial \theta}])] \quad (14)$$

$$- \frac{1}{r \sin \theta} (\frac{\partial}{\partial r}(r \sin \theta [u_r B_\theta - \frac{\eta}{r} (\frac{\partial}{\partial r}(rB_\theta) - \frac{\partial B_r}{\partial \theta})]) = 0 \quad (15)$$

$$\frac{1}{r} [\frac{\partial}{\partial r}(r u_\varphi B_r) + \frac{\partial}{\partial \theta}(u_\varphi B_\theta)] = 0 \quad (16)$$

Now we have a set of MHD equations which describe the dynamical behavior of magnetized ADAFs. The solution of these equations are strongly depends on viscosity, resistivity, degree of advection and the role of thermal conduction on the disks.

These nine partial differential equations governing the non-self gravitating, magnetized advection dominated viscose flows. These equations relate 15 dependent variables:  $p, \rho, \epsilon, \mu, \mu_b, \eta$  and the components of  $\mathbf{u}, \mathbf{J}$  and  $\mathbf{B}$ . For the set of equations, we use the following standard assumptions:

The kinematic viscosity coefficient,  $\nu = \frac{\mu}{\rho}$ , is generally parameterized using the  $\alpha$ -prescription (Shakura-Sunyaev 1973),

$$\nu = \alpha c_s H, \quad (17)$$

where  $H = \frac{c_s}{\Omega_k}$  is known as the vertical scale height,  $c_s = \sqrt{\frac{p}{\rho}}$  is the isothermal sound speed and the dimensionless coefficient  $\alpha$  is assumed to be independent of  $r$ . So, we introduce the parameter  $\eta$  as the magnetic diffusivity and insert it as a constant parameter in our equations. Both the kinematic viscosity coefficient  $\nu$  and the magnetic diffusivity  $\eta$  have the same units and are assumed to be due to turbulence in the accretion flow. Thus it is physically reasonable to express  $\eta$  such as  $\nu$  via the  $\alpha$ -prescription of Shakura-Sunyaev (1973) as follows (Bisnovaty-Kogan & Ruzmaikin 1976),

$$\eta = \eta_0 c_s H. \quad (18)$$

To determine thermodynamical properties of the flow in the energy equation, we require a constitutive relation as a function of two state variables. Therefore we choose an equation for the internal energy as  $\epsilon = \frac{p}{\rho(\Gamma-1)}$  where  $\Gamma$  is the ratio of specific heats of the gas.

To satisfy  $\nabla \cdot \mathbf{B} = 0$ , we may introduce a convenient functional form for the magnetic field. Owing to the axisymmetry, the magnetic field can be written as

$$\mathbf{B} = \mathbf{B}_p(r, \theta) + B_\phi(r, \theta) \mathbf{e}_\phi \quad (19)$$

Angular momentum is expected to be carried away from the disk by magnetic stresses along the externally given poloidal magnetic lines of force. In the case of dipole-type external field it is transferred to the central accretor (Kaburaki, 2000). The effect of magnetic diffusivity on magnetically driven mass accretion was studied by Kaburaki (2000). They showed that the effects of resistivity are that magnetic field lines do not rotate with the same angular speed as the disk matter and thus it suppresses the injection of magnetic helicity and magneto-centrifugal acceleration. So, by neglecting the toroidal component of the field,  $B_\phi$ , we can express the poloidal component,  $\mathbf{B}_p$ , in terms of a magnetic flux function  $\Psi(r, \theta)$ :

$$\mathbf{B} = \mathbf{B}_p(r, \theta) = \frac{1}{2\pi} \nabla \times \left( \frac{\Psi}{r \sin \theta} \mathbf{e}_\phi \right) \quad (20)$$

It is clear that the basic equations are nonlinear and we

cannot solve them analytically. Therefore, it is useful to have a simple means to investigate the properties of solutions. We seek self-similar solution for the above equations. In the next section we will present self-similar solutions of these equations.

### 3 SELF-SIMILAR SOLUTIONS

To understand better the physical processes of our viscous-resistive ADAF accretion disks, we seek self-similar solutions of the above equations. The self-similar method is familiar from its wide applications to the full set of MHD equations. The self-similar method is not able to describe the global behavior of accretion flows, because no boundary condition has been taken into account. However, as long as we are not interested in the behavior of the flow near the boundaries, such solutions are very useful.

Writing the equations in non-dimensional forms, that is, scaling all the physical variables by their typical values, bring out the non-dimensional variables. We can simply show that the solutions of the following forms, satisfy the equations of our model:

$$\rho(r, \theta) = \rho_o \rho(\theta) (r/r_o)^{-3/2}, \quad (21)$$

$$p(r, \theta) = p_o P(\theta) (r/r_o)^{-5/2}, \quad (22)$$

$$u_r(r, \theta) = r \Omega_K(r) U(\theta), \quad (23)$$

$$u_\varphi(r, \theta) = r \sin \theta \Omega_K(r) \Omega(\theta), \quad (24)$$

$$B_r(r, \theta) = \frac{B_o}{2\pi \sin \theta} \frac{d\Psi(\theta)}{d\theta} (r/r_o)^{-5/4}, \quad (25)$$

$$B_\theta(r, \theta) = -\frac{3B_o \Psi(\theta)}{8\pi \sin \theta} (r/r_o)^{-5/4}, \quad (26)$$

where  $\rho_o$ ,  $p_o$ ,  $B_o$  and  $r_o$  provide convenient units with which the equations can be written in non-dimensional forms. Substituting the above solutions in the equations (10)-(16), we obtain a set of coupled ordinary differential equations in terms of  $\theta$ .

$$\begin{aligned} \frac{dP}{d\theta} &= \frac{3\alpha P}{2(1-\alpha U)} \frac{dU}{d\theta} + \frac{3\rho K U}{16\pi^2 \beta_o \eta_o c_1 P \Omega^2 \sin^2 \theta (1-\alpha U)} \frac{d\Omega}{d\theta} \\ &+ \frac{\rho \Omega^2 \sin \theta \cos \theta}{c_1 (1-\alpha U)} \end{aligned} \quad (27)$$

$$\begin{aligned} \frac{d^2 U}{d\theta^2} &= -\frac{2.5}{\alpha} - U - \cot \theta \frac{dU}{d\theta} - \frac{1}{P} \frac{dP}{d\theta} \frac{dU}{d\theta} \\ &+ \frac{\rho}{c_1 \alpha P} \left(1 - \frac{U^2}{2} + \Omega^2 \sin^2 \theta\right) + \frac{2UK\rho}{\beta_o \eta_o \alpha c_1 \Omega} \left(\frac{3}{8\pi \rho \sin \theta}\right)^2 \end{aligned} \quad (28)$$

$$\begin{aligned} \frac{d\rho}{d\theta} &= \frac{2}{5} \frac{c_1^{-1/2} P^{-1/2} \rho^{3/2}}{\phi_s} \left[ \frac{U(3\gamma-5)}{2(\gamma-1)} - \alpha f (3U^2 + \left(\frac{dU}{d\theta}\right)^2) + \frac{9}{4} \Omega^2 \right. \\ &\left. \sin^2 \theta + \left(\frac{d\Omega}{d\theta}\right)^2 \sin^2 \theta \right] - \frac{2}{5} \frac{f c_2 \eta_o c_1^{-5/2} P^{-5/2} \rho^{5/2} K}{16\pi^3 \phi_s \Omega} \left(\frac{3U}{4\eta_o \sin \theta}\right)^2 \\ &- 2(1 - \cot \theta) \rho + 3 \frac{\rho}{P} \frac{dP}{d\theta} \end{aligned} \quad (29)$$

$$\frac{d\Omega}{d\theta} = \frac{-A \pm \sqrt{A^2 + 3B}}{3} \quad (30)$$

Finally, by definition  $\beta_o = \frac{P_o}{B_o^2/8\pi}$ ,  $\Omega \Psi^2 = K$ , where  $K$  is an arbitrary constant, so  $c_1 = \frac{p_o}{\rho_o} \left(\frac{GM}{r_o}\right)^{-1} = \frac{2p_o}{\rho_o u_{ff}^2}$  and

$$c_2 = \frac{B_o^2}{\rho_o} \left(\frac{GM}{r_o}\right)^{-1}.$$

In equation (30) we have the followings:

$$A = \frac{\Omega}{P} \frac{dP}{d\theta} + 4\Omega \cot \theta,$$

$$B = \left[ \frac{9}{4} + \left(\frac{1}{\alpha} + \frac{3}{\eta_o}\right) \frac{\rho U}{c_1 P} \right] \Omega^2,$$

Equations 27-30 constitute a system of ordinary non-linear differential equations for the four self-similar variables  $\Omega$ ,  $P$ ,  $U$  &  $\rho$ .

There are many techniques for solving these nonlinear equations. Analytical methods can yield solutions for some simplified problems. But, in general this approach is too restrictive and we have to use the numerical methods. Here, one can employ the method of relaxation to the fluid equations (Press et al. 1992). In this method we replace ordinary differential equations by approximate finite-difference equations on a grid of points that spans the domain of interest. The relaxation method determines the solution by starting with a guess and improving it, iteratively. Based on it, this system of equations can be solved for all unknowns as a function of  $\theta$ , once we are given a set of boundary conditions where constraints are placed on the flow. The boundary conditions are distributed between the equatorial plane,  $\theta = \frac{\pi}{2}$  and the rotation axis,  $\theta = 0$ . We can use Narayan & Yi (1995) Boundary conditions in both boundaries: the boundary conditions at  $\theta = 0$

$$\frac{dU}{d\theta} = \frac{d\Omega}{d\theta} = \frac{dP}{d\theta} = \frac{d\rho}{d\theta} = 0 \quad , \quad U = 0, \rho = 0, \quad (31)$$

and in this method the boundary conditions at  $\theta = \frac{\pi}{2}$  are:

$$\frac{dU}{d\theta} = \frac{d\Omega}{d\theta} = \frac{dP}{d\theta} = \frac{d\rho}{d\theta} = 0. \quad (32)$$

The boundary conditions on the above equations require that variables are assumed to be regular at the endpoints. Also the net mass accretion rate (9) provides one boundary condition for  $\rho$ :

$$\int_0^{\frac{\pi}{2}} \rho(\theta) U(\theta) \sin \theta d\theta = -\frac{1}{2}$$

We obtain numerical solutions for the flows with fixed values of  $\eta_o = 0.1$ ,  $\Gamma = \frac{4}{3}$ ,  $\alpha = 0.01, 0.05, 0.1$ ,  $f = 0.1, 0.3, 0.7$  and  $\phi_s = 0.001, 0.007, 0.01$ . We consider  $c_1 = 0.8$ ,  $c_2 = 2 \times 10^3$  and  $\beta_o = 0.01$  (Ghanbari , Salehi & Abbassi 2007)

### 4 RESULTS

We have obtained numerical solutions of equations (27)-(30) for a variety of viscosity,  $\alpha$ , advection,  $f$  and the thermal conduction  $\phi_s$  parameters. The three panels in Figure 1 show the variations of various dynamical quantities in terms of polar angle  $\theta$  for with a fixed values of viscosity and thermal conduction parameters with a sequence of increasing advection parameter  $f$ . The top panel displays the dimensionless radial velocity  $U(\theta)$ .  $U(\theta)$  is zero at  $\theta = 0$  (this is a boundary

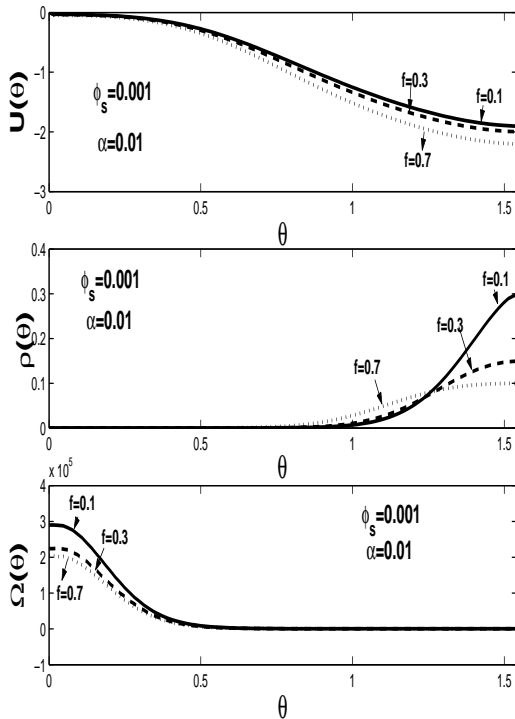


**Figure 1.** The self-similar solutions of radial velocity  $U(\theta)$  (top), density  $\rho(\theta)$  (middle) and angular velocity  $\Omega(\theta)$  (bottom) as a function of polar angle  $\theta$  corresponding to  $\Gamma = 4/3$ ,  $\eta_0 = 0.1$ ,  $\beta_0 = 0.01$  and  $f = 0.1, 0.3, 0.7$  for  $\alpha=0.1$  and  $\phi_s = 0.001$

condition) and maximum at  $\theta = \frac{\pi}{2}$ . Thus, the inflow velocity reaches its maximum in the equatorial plane and vanishes along the polar axis. As expected, the velocity is sub-Keplerian. The middle panel shows the density profile  $\rho(\theta)$  of the solutions. The density contrast in the equatorial and polar regions increases with a decrease in the advection parameter  $f$ . For a given  $\alpha$  and  $\phi_s$ , solutions with small values of  $f$  behave like standard thin disks, as might be expected, these solutions correspond to  $f \rightarrow 0$  and so a small fraction of energy would be advected. In the opposite,  $f \rightarrow 1$ , advection-dominated limit, our solutions describe nearly spherical flows which rotate far below the Keplerian velocity. The bottom panel shows the profile of the angular velocity  $\Omega(\theta)$ .  $\Omega(\theta)$  decreases increase in the advection in the accretion disks. We find that in the inner boundary,  $U(\theta)$  is essentially independent of advection parameter  $f$ . But in intermediate values of  $\theta$ , the radial velocity is modified by  $f$ ; in the Shadmehri's solutions (2004), two distinct regions in the  $U(\theta)$  profile could be recognized. The bulk of accretion occurs from equatorial plane at  $\theta = \frac{\pi}{2}$  to  $\theta = \theta_s$ , in which the radial velocity is zero. While in Narayan & Yi solutions, there is no zero inflow in  $0 < \theta < \frac{\pi}{2}$ . Our solutions show that in any given  $\theta$  the radial velocity is nonzero and when we increase the advection parameter the radial velocity will be increased.

Here we may comment about the fact that when the advection parameter,  $f$ , goes to zero, our disk dose not correspond to a globally cooling flow, because of the appearance of thermal conduction term in the energy transport equa-

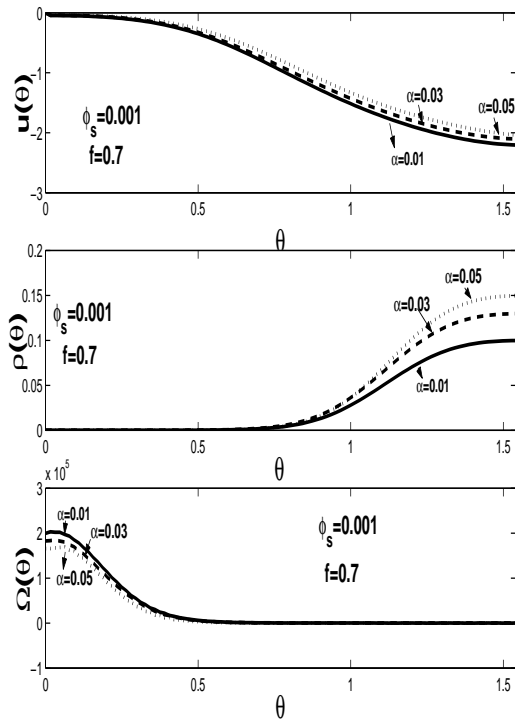


**Figure 2.** The self-similar solutions of radial velocity  $U(\theta)$ (top) and density  $\rho(\theta)$  (middle) and angular velocity  $\Omega(\theta)$  (bottom) as a function of polar angle  $\theta$  corresponding to  $\Gamma = 4/3$ ,  $\eta_0 = 0.1$ ,  $\beta_0 = 0.01$  and  $\alpha = 0.01, 0.03, 0.05$  for  $f = 0.7$   $\phi_s = 0.001$

tion. When  $f$  goes to 1 our disks are not fully advective, because some part of the energy generated by viscosity will be transported by thermal conduction.

Figure 2 displays the behavior of radial and angular velocities and density profile for different values of the viscosity parameter for fixed advection and thermal conduction parameters. We find that the value of viscous parameter,  $\alpha$ , affects quantitatively (but not qualitatively) on the dynamical variables of the accretion flow. For the larger value of the viscous parameter, the radial inflow decreases and the density would be increased overall, which is compatible with the results presented by Ghanbari et al (2007).

Three panels in Figure 3 show, for fixed advection and viscosity parameters with a sequence of thermal conduction parameters,: (1) The radial velocity increases with an increase in the thermal conduction parameter (2) The density profile increases with a decrease in the thermal conduction parameter (3) The angular velocity decreases with an increase in the  $\phi_s$  in the accretion discs.

In Fig. 4 we display the isodensity contours in the meridional plane. The top, middle and bottom panels display the isodensity profiles for different values of conduction, advection and viscous parameters, respectively. The panels in figure 4 show that the disk seems to be thick. Solution with the same  $f$  but for different values of  $\alpha$  are distinguishable from one another. By adding viscous parameter the geometrical shape of the disc becomes thick more and more. This advection-dominated solutions have very similar

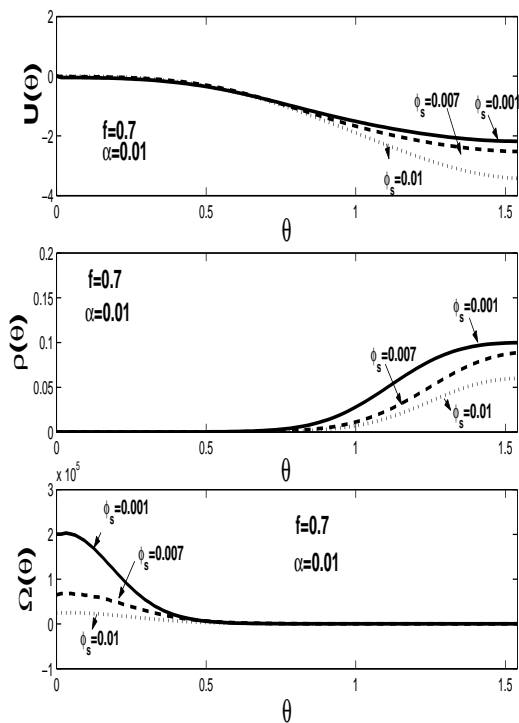


**Figure 3.** The self-similar solutions of radial velocity  $U(\theta)$ (top) and density  $\rho(\theta)$  (middle) and angular velocity  $\Omega(\theta)$  (bottom) as a function of polar angle  $\theta$  corresponding to  $\Gamma = 4/3$ ,  $\eta_0 = 0.1$ ,  $\beta_0 = 0.01$  and  $\phi_s = 0.001, 0.007, 0.01$  for  $f = 0.7$   $\alpha = 0.01$

properties to the approximated solution derived by Narayan & Yi (1994), Ghanbari et al (2007) and Shadmehri (2004).

The overall structure of the dynamical variables remain very close to the original 2D ADAF solutions of Narayan & Yi (1995). This solution is denser close to the equator than at the pole, and it is some thing like a "thin disk" surrounded by a hot coronal atmosphere.

As the values of  $\phi_s$  are increased, the solutions substantially start to deviate from standard solutions, with faster radial flow and rotating more slowly (becomes more pressure supported) in the equator. By increasing  $\phi_s$ , density reduces in the equatorial plane, and the density profile becomes more uniform. It gradually approaches to the spherically symmetry. This behavior of the solutions are shared by original ADAFs solutions and Ghanbari et al.'s work (2007)

## 5 SUMMERY AND CONCLUSION

The main aim of this investigation was to obtain an axi-symmetric self-similar advection-dominated solution for viscous-resistive accretion flow with the poloidal magnetic field in the presence of thermal conduction. Using the basic equations of fluid dynamics in spherical polar coordinates  $(r, \theta, \varphi)$ , we have found the self-similar solutions for thick discs to derive a set of coupled differential equations that govern the dynamics of the system. We have then solved the equations using the relaxation method by considering boundary conditions and using the  $\alpha$ -prescription (Shakura

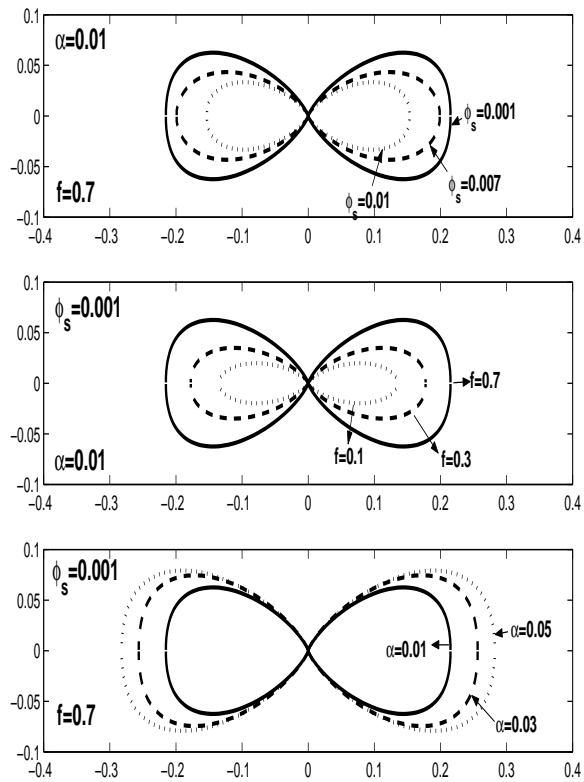


**Figure 4.** isodensity contours for  $\Gamma = 4/3$ ,  $\eta_0 = 0.1$ ,  $\beta_0 = 0.01$  and  $\phi_s = 0.001, 0.007, 0.01$  for  $f = 0.7$   $\alpha = 0.01$ (top) and  $f = 0.1, 0.3, 0.7$  for  $\alpha=0.01$  and  $\phi_s = 0.001$ (middle) and  $\alpha = 0.01, 0.05, 0.1$  for  $f = 0.7$   $\phi_s = 0.001$  (bottom)

& Sunyaev, 1973) in order to extract some of the similarity functions in terms of the polar angle  $\theta$ .

We showed that the radial and rotational velocities are well below the Keplerian velocity. The Bulk of accretion with nearly constant velocity occurs in the regions which extend from equatorial plane to a given  $\theta$  which highly depends on advection parameter  $f$ . In a non-advective regime, low  $f$ , we have a standard thin accretion disk, but for a high  $f$  the accretion is nearly spherical.

It is difficult to evaluate the precise picture of radiative inefficient accretion flow in the presence of thermal conduction with a self-similar method. But this method can reproduce overall dynamical structure of the disks with a set of given physical parameters. Even though, conduction heats up the accretion flows locally, the reduced density resulting from the larger inflow velocity, leads a net decrease in the expected level of free-free emissions. The very steep dependence of synchrotron emissions on the electron temperature (e.g. Mahadevan & Quataret 1997), suggests that hotter solutions (with conduction) maybe more efficient radiatively (Tanaka & Menou 2006). From self-similar solutions alone, we can determine how the global structure of the flow can be affected by thermal conduction. For small enough values of  $\phi_s$  the solutions remain very close to the Ghanbari et al. (2007) solutions. The main difference between their solution with standard solution of 2D ADAFs of Narayan & Yi (1995a) is the presence of dipolar magnetic field and its correspond resistivity. In our case, we add extra physics by adding the thermal conduction as a mechanism for energy

transport. By adding the thermal conduction the solution start deviating substantially from the original ADAFs, with faster radial inflow at the equator. These results well agree with Tanaka & Menou (2006).

The presence of magnetic field with the poloidal configuration will affect the role of thermal conduction. Compare to non-magnetic field solution, (Tanaka & Menou 2006) in our case the existence of magnetic resistivity can produce more energy to be advected. The B-field configuration can also affect the energy transportation along the accretion disks. However, the main aim of this work is to study the quasi-spherical magnetized flow, directly by solving the relevant MHD equations. Although, we have made some simplifications in order to treat the problem analytically, our self-similar solutions show that the input parameters, such as thermal conduction and viscose parameters, magnetic field and its resistivity can really change typical behavior of the physical quantities of the ADAF disks. Of course, our self-similar solutions are too simple to make any comparison with observations. But, we think one may relax self-similarity assumptions and solve the equations of the model numerically. This kind of similarity solutions can greatly facilitate testing and interpreting the results.

## 6 ACKNOWLEDGMENTS

We are grateful to the referee for a very careful reading of the manuscript and for his/her suggestions, which have helped us improve the presentation of our results.

## REFERENCES

- Abramowicz M.A., Czerny B., Lasota J.P., Szuszkiewicz E., 1988, ApJ, 332, 646  
 Abramowicz M.A., Chen X., Kato S., Lasota J.P., Regev, O., 1995, ApJ, 438, L37  
 Abbassi S., Ghanbari J., Najjar S., 2008, MNRAS, 388, 663  
 Abbassi S., Ghanbari J., Salehi F., 2006, A&A, 460, 357  
 Bisnovatyi-Kogan G.S., Ruzmaikin A.A., 1976, Ap&SS, 42, 401  
 Bisnovatyi-Kogan G.S., Lovelace, R.V.E., 2000, ApJ, 529, 978  
 Cowie, L. L., Mackee, C.F., 1977, ApJ, 275, 641  
 Ghanbari J., Salehi F., Abbassi S., 2007, MNRAS, 381, 159  
 Hameury J.M., Lasota J.P., Maclintock J.E., Narayan R., 1997, ApJ, 489, 234  
 Honma, F., 1996, PASJ, 48, 77  
 Ichimaru, S. 1977, ApJ, 214, 840  
 Johanson, B.M., Quataert, E., 2007, ApJ, 660, 1273J  
 Kaburaki, O. 2000, ApJ, 531, 210  
 Lasota, J. P., Abramowicz, M. A., Chen, X., Krolik, J., Narayan, R., Yi, I, 1996, ApJ, 462, 142  
 Mahadevan, R., Quataert, E., 1997, ApJ, 490, 605  
 Manmoto, T., Kato, S., Nakamura, K., Narayan, R., 2000, APJ, 529, 127  
 Mihalas D., Mihalas B.W., 1984, Foundation of Radiation Hydrodynamics, Oxford Univ. Press, New York  
 Narayan, R., & Yi, I. 1994, ApJ, 428, L13  
 Narayan, R., & Yi, I. 1995a, ApJ, 444, 238  
 Narayan, R., & Yi, I. 1995b, ApJ, 452, 710  
 Narayan, R., Maclintock, J.E., Yi, I., 1996, ApJ, 457, 821  
 Narayan, R., Igumenshchev, I.V., Abramowicz M.A., 2000, ApJ, 539, 798  
 Press, W. H., Teukolsky, S. A., Vetterling, W. T., & Flannery, B. P. 1992, Numerical Recipes.  
 Shadmehri, M. 2004, A&A, 424, 379  
 Shadmehri, M. 2008, AP&SS, 317, 201S  
 Shakura, N. I., & Sunyaev, R.A. 1973, A&A, 24, 337  
 Shapiro, S., Lightman, A.P., Eardley D.M., 1976, ApJ, 204, 187  
 Tanaka, T., Menou, K., 2006, APJ, 649, 345